

Utilization of Residual Helium to Extend Satellite Lifetimes and Mitigate Space Debris

Mitchell L. R. Walker*

Georgia Institute of Technology, Atlanta, Georgia 30332

Ryan P. Russell†

The University of Texas at Austin, Austin, Texas 78712-0235

and

Lake A. Singh‡

Georgia Institute of Technology, Atlanta, Georgia 30332

DOI: 10.2514/1.B34498

A new electric propulsion device concept takes advantage of residual helium gas that is trapped in the chemical propellant feed system and currently unused at end of life. The helium ion thruster provides additional propellant resources to extend satellite lifetimes and transfer geostationary orbit space assets to ultrasafe disposal orbits. The predicted capability, if fully allotted to the disposal, allows for perigee heights above the geostationary altitude that are one order of magnitude greater than existing international guidelines of ~250 km. Furthermore, the proposed helium ion thruster concept makes the classic propellant gauge uncertainty problem moot, as satellite operators could use all of their conventional propellant for nominal station-keeping operations. The helium ion thruster concept therefore mitigates future space debris arising from depleted assets in the geostationary orbit belt through both aggressive orbit raising and depressurization of satellites at end of life. An analysis of the helium ion thruster theoretical performance shows that the device could raise the altitude of an end-of-life 2500 kg, 5 kW spacecraft by 2200 km in two months using 2 kg of residual helium.

Nomenclature

a	=	semimajor axis, m
e	=	electron charge, C
g_0	=	gravitational acceleration at Earth's surface, m/s ²
H.O.T.	=	higher-order terms
I_{sp}	=	specific impulse, s
I_{sp}^*	=	specific impulse of an alternative thruster, s
m	=	propellant molecular mass, spacecraft mass, kg
m_{HT}	=	dry mass of helium ion thruster, kg
m_0	=	pre-disposal-maneuver mass, kg
m_p	=	propellant mass, kg
P_{input}	=	power supplied to the thruster, W
$P_{ionization}$	=	power required to ionize the propellant, W
P_{other}	=	power consumed by losses, W
P_{thrust}	=	jet power from the exhaust flow, W
r	=	orbit radius, m
r_b	=	burnout radius, m
t	=	time, s
V_B	=	beam voltage, V
V_{NC}	=	neutralizer coupling voltage, V
v	=	velocity, m/s
γ	=	efficiency factor accounting for beam divergence and double ion production

Δ	=	ratio of propellant and pre-disposal-maneuver masses
δ_{vH}	=	Hohmann velocity increment, m/s
ε	=	ion production cost, eV
η	=	thrust efficiency
η_u	=	propellant utilization efficiency
κ	=	ratio of I_{sp} for the helium ion thruster and a nominal thruster
μ	=	gravitational parameter of Earth, m ³ /s ²
ξ	=	efficiency

I. Introduction

UNCERTAINTY in propellant reserve estimations, financial pressures, and lack of regulatory requirements have led to an alarmingly low success rate of geostationary Earth orbit (GEO) satellites reaching proper disposal orbits at end of life (EOL). Space debris hazards to assets in the GEO belt continue to increase in part due to this low success rate. The combination of the extraordinary value of GEO satellites, the crowded nature of GEO slots, and recent studies have highlighted that the space debris problem at GEO is of great concern to the entire space community [1–3]. Nearly half of all currently operating spacecraft are in the GEO environment [2]. Almost 20% of objects near GEO are abandoned assets drifting in all longitudes of the protected GEO ring while many intrude daily into the protected region [3]. A recent paper [2] argues that explosions in GEO are the greatest debris risk and suggests that the EOL guideline “does not improve the situation much, because even just a dozen explosions would be sufficient to double the average flux of debris. . . thus matching the effect of the existing background. . . a re-orbiting altitude at least 2000 km above GEO should be used.”

Currently, the U.S. Space Object Catalog lists approximately 15,000 trackable objects accounting for approximately 5800 tons of on-orbit mass. The total debris population is thought to exceed 20,000 objects larger than 10 cm [4]. The catalogue maintenance problem is already an international concern of extraordinary size and complexity, and its scope is somewhat unbounded with the potential for exponential growth. Figure 1 shows the growth of trackable objects by category over the history of spaceflight. The evolution of

Received 7 November 2011; revision received 16 May 2012; accepted for publication 18 May 2012. Copyright © 2012 by Mitchell Walker, Ryan P. Russell, and Lake Singh. Published by the American Institute of Aeronautics and Astronautics, Inc., with permission. Copies of this paper may be made for personal or internal use, on condition that the copier pay the \$10.00 per-copy fee to the Copyright Clearance Center, Inc., 222 Rosewood Drive, Danvers, MA 01923; include the code 0748-4658/12 and \$10.00 in correspondence with the CCC.

*Associate Professor, Department of Aerospace Engineering, 270 Ferst Drive NW, Associate Fellow AIAA.

†Assistant Professor, Department of Aerospace Engineering and Engineering Mechanics, 210 E. 24th St. Stop C0600, Austin, TX 78712-1221; ryan.russell@austin.utexas.edu. Senior Member AIAA.

‡Graduate Student, Department of Aerospace Engineering, 270 Ferst Drive NW, Student Member AIAA.

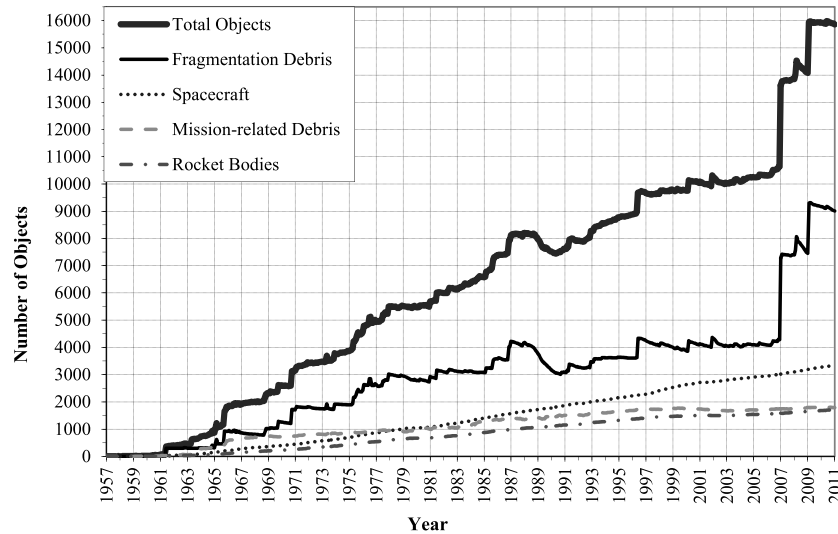


Fig. 1 Evolution of trackable objects during the space age. Fragmentation debris has increased dramatically in recent years [5].

fragmentation debris indicates the recent growth of hazardous objects and highlights the potential for exponential growth. Although the space debris problem is conventionally considered to be of greater concern in low Earth orbit (LEO) due to higher velocities and compact orbit geometry, the threat of space debris is present both in LEO and in GEO.

A recent survey found that 17% of the 869 objects near GEO are abandoned assets drifting in all longitudes of the protected GEO ring. Of the 48% drifting above GEO, many intrude daily into the protected region [3]. Despite the improved awareness in recent decades of the potential hazards of space debris, just under half of the decommissioned GEO satellites in 2005, and only 39 out of 117 in the years between 1997 and 2004, followed the recommended EOL guidelines. A recent paper [2] studies the orbit evolution of large area-to-mass particles and finds alarming growth in eccentricity that quickly endangers the protected GEO regions. Such high area-to-mass particles are unfortunate artifacts of explosions and collision events.

A number of recent events have made space debris a critical issue. In 2010, Intelsat lost control of the Galaxy 15 GEO satellite. Currently, satellite operators are using propellant budgets on the active assets near Galaxy 15 to prevent a collision. However, if the rogue, fully fueled Galaxy 15 satellite collides with an inactive, indisposed GEO satellite, the results could be catastrophic to users of geosynchronous orbits. Future control failures of GEO space assets will only aggravate this situation.

Of the space-faring nations, only the United States and the former Soviet Union, until recently, had demonstrated the ability to destroy space assets with surface-based missiles. In 2007, China became the third nation to demonstrate antisatellite technology, and in doing so generated significant space debris, causing concern to the international space community [6]. The China antisatellite test demonstrated the unstable nature of the space debris environment; the antisatellite test nearly doubled the number of trackable fragmentation debris, thus significantly increasing the risk of unintentional destruction of other assets.

The unintentional destruction of U.S. space assets due to space debris has become a reality. In February 2009, a U.S. Iridium satellite was destroyed in an unprecedented collision with an expended Russian satellite. As new space assets are added to the high-value orbits and old assets remain in close proximity, satellite collisions will become more common. If steps are not taken to mitigate the problem, some researchers have predicted a cascading of collisions that is very difficult if not impossible to stop [7].

The potential for loss of life as a result of space debris is present and real. Twice since the February 2009 collision, the crew of the International Space Station (ISS) has been forced to evacuate to the Soyuz modules as a result of close encounters with large pieces of

debris [8,9]. The Space Shuttle had numerous encounters over the course of its operation with small pieces of debris which damaged windows and thermal protection tiles critical for safe reentry [10]. In June 2011, the ATV-2 cargo resupply craft was forced to perform a collision-avoidance maneuver after undocking with the ISS because NASA predicted a collision event with a miss distance of 50 m. Had a collision occurred so close to the ISS, the resulting debris field could have critically damaged or even destroyed the station. The continued growth of the number of debris objects coupled with increased human presence in space could prove to be a lethal combination. Clearly, solutions are needed to mitigate and reverse this growing problem.

In this study, a supplementary EOL propellant system is proposed as a debris-mitigation solution in the GEO environment. The novel electric propulsion (EP) device uses residual helium gas trapped in the chemical propellant feed systems that are currently used for chemical-thruster-driven geostationary transfer orbits. The proposed system also provides valuable extensions to satellite lifetimes by allowing operators to use the entirety of their station-keeping propellant on nominal operations. At EOL, the system exploits the currently unused helium residuals to transfer the GEO satellite to a safe graveyard disposal orbit. Preliminary analyses suggest that an altitude up to ~ 2000 km above GEO is achievable for the representative GEO spacecraft considered. The EP device is termed a helium ion thruster (HIT) and is a concept to mitigate space debris. The helium ions are electrostatically accelerated with biased grids to generate thrust. The use of the helium-fed EP device significantly reduces the threat of space debris in precious GEO slots by moving expended assets a safe distance from active assets in the GEO belt (mitigating collision risk) and actively depressurizing the chemical feed system (mitigating explosion risk). Furthermore, the HIT device will maximize nominal lifetime operations and has the potential to bring cost and performance value to government and commercial space operations.

II. Previous Work

To date, most developed thrusters that use helium as a propellant are the microwave electrothermal thruster (MET) and the arcjet [11,12]. These thruster designs achieve the acceleration of their propellant gas by the addition of heat: electrothermal propulsion. The development of the MET originated at Michigan State University in the early 1980s [13]. The Michigan State University investigation was shortly joined by researchers from Pennsylvania State University [14]. Into the 1990s, NASA tested scaling up the power, and the Aerospace Corporation continued to support development [15]. The MET operating on helium has demonstrated a maximum I_{sp} of 1330 s [16] and efficiency ranges from 60 to 75% [15]. Well

before the envisioning of the MET, the idea of using helium in an arcjet was raised in the early 1960s. Although helium is a heavier atom than hydrogen, it is monatomic, and thus it is less prone to frozen flow losses [17]. The helium arcjet design has achieved a maximum specific impulse I_{SP} of 760 s and thrust of 112 mN at a thrust efficiency of 50.2% [18].

To date, helium-fed EP devices have not been used on space assets for a number of reasons. First, the theoretical ionization energy of helium is 24.6 eV, which is the highest ionization energy of all the elements. It is more than two times greater than that of xenon (12.1 eV), the most common EP propellant. This means that a significant amount of energy is wasted in the ionization process. On past low-power (<5 kW) satellites, the use of low-efficiency devices was not an option. Current and future generations of GEO satellites will operate at much higher powers (10–30 kW). Second, helium has an extremely small ionization cross section. The small ionization cross section results in a lower ionization rate of the propellant [19]. Thus, even if sufficient power is available, standard electrostatic EP devices cannot effectively use helium as a propellant.

The high ionization cost of helium leads to very low (<10%) electrostatic propulsion efficiency. Low efficiency requires high power to generate appreciable thrust, which until the last decade was not available at EOL. As of 2011, in an EOL GEO satellite application, engine efficiency is not a mission driver because the satellite has on the order of 10 kW of electrical power available with minimal payload demands. The driver at EOL is I_{SP} because it determines the maximum velocity increment that the vehicle can obtain. Thus, the low molecular weight and extremely high I_{SP} of an HIT system are well-suited to GEO EOL applications.

III. Proposed Concept and Expected Performance

For a helium-fed EP device to deliver the most substantial velocity increment to a GEO size communications satellite, a high I_{SP} in the range of 5000 to 11,000 s is desired, which can only be achieved with electrostatic acceleration. The arcjet and MET concepts are insufficient for this level of performance. The next section details the expected performance of the proposed HIT device using helium.

A. Expected Performance

1. Helium as a Propellant

For a given electrostatic acceleration voltage (typically between 20 and 500 V), helium will have a higher ion velocity than xenon as a result of their difference in mass. Consequently, a higher I_{SP} is attainable with helium than with xenon at the same acceleration voltage. In contrast, the efficiency of EP devices running helium is not as favorable due to the high ionization cost of the propellant. However, for this novel EOL application, the system can tolerate low thrust efficiency as long as the propellant utilization and I_{SP} remain

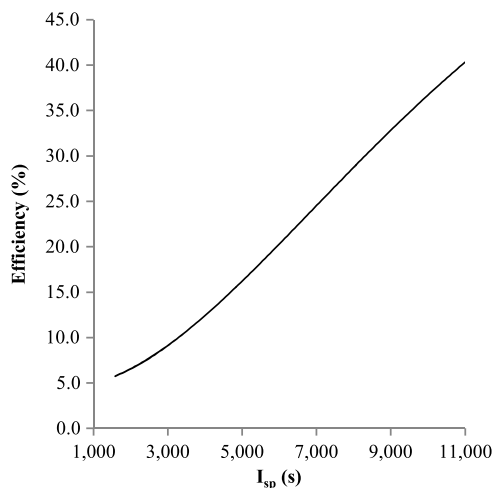


Fig. 2 Expected helium-fed thruster efficiency curve as a function of specific impulse.

Table 1 Parameters and assumptions for efficiency curve

Description	Value
Molar mass (He)	4.003 g/mol
Neutral mass (He)	6.64714E – 27 kg
Ion mass (He ⁺)	6.64714E – 27 kg
Ion charge	1.6E – 19 C
Ionization energy (He)	24.587 eV
Approximate ionization cost (He ⁺)	246 eV
Cathode-to-ground	15 V
Propellant utilization	0.9
Beam divergence	0.95

high. The low thrust efficiency is tolerable because, at EOL, the satellite has a significant amount of excess electrical power. Figure 2 illustrates the expected efficiency as a function of I_{SP} for helium considering a range of acceleration voltages spanning from 20 to 260 V. The figure indicates an I_{SP} range of ~1000 to 11,000 s for the given range of acceleration voltages. The parameters and assumptions that fed into the computation of the efficiency curve are summarized in Table 1. The parameters are conservative estimates based on existing EP technology.

In its most fundamental form, the thrust efficiency η is defined in Eq. (1), where P_{thrust} is the jet power from the exhaust flow, and P_{input} is the electrical power supplied to the HIT. Equation (2) shows that P_{input} is composed of jet power, $P_{ionization}$ the power required to ionize the propellant, and P_{other} , which includes losses due to processes such as radiation. If we consider P_{other} to be small in comparison to P_{thrust} and $P_{ionization}$, then Eq. (1) is equivalent to Eq. (3) [20], where η_u is the propellant utilization, γ is an efficiency factor that accounts for beam divergence and double ion production, ε is the ion production cost, V_{NC} is the neutralizer coupling voltage, and V_B is the beam voltage. The beam divergence and double ion production factor accounts for energy lost from ion trajectories not along the thrust vector and energy lost from stripping excess electrons from some ions. Equation (3) reveals the intuitive result that the thrust efficiency is maximized when the power required to ionize each atom is minimized. The I_{SP} as a function of discharge voltage is given by Eq. (4) [20], where e is the electron charge, m is the atomic mass of the propellant, and g is gravity. Equation (4) can be substituted into Eq. (3) to yield Eq. (5), which gives the efficiency as a function of I_{SP} :

$$\eta \equiv \frac{P_{thrust}}{P_{input}} \quad (1)$$

$$P_{input} \equiv P_{thrust} + P_{ionization} + P_{other} \quad (2)$$

$$\eta = \frac{\eta_u \gamma^2}{1 + \frac{\varepsilon + V_{NC}}{V_B}} \quad (3)$$

$$I_{SP} = \frac{\sqrt{2e(V_B - V_{NC})}}{g_0} \quad (4)$$

$$\eta = \frac{\eta_u \gamma^2}{1 + \frac{\varepsilon + V_{NC}}{\frac{e}{2e}(I_{SP} g_0)^2 + V_{NC}}} \quad (5)$$

By integrating the results of this efficiency analysis in with a continuous thrust model, an estimate of the orbit-raising capability of the HIT can be determined.

2. Continuous Thrust Model

Starting from the Gauss form of the Lagrange planetary equations, the time rate of change for a spacecraft's semimajor axis is known [21] to be

$$\frac{da}{dt} = \frac{2va^2 T}{\mu m} \quad (6)$$

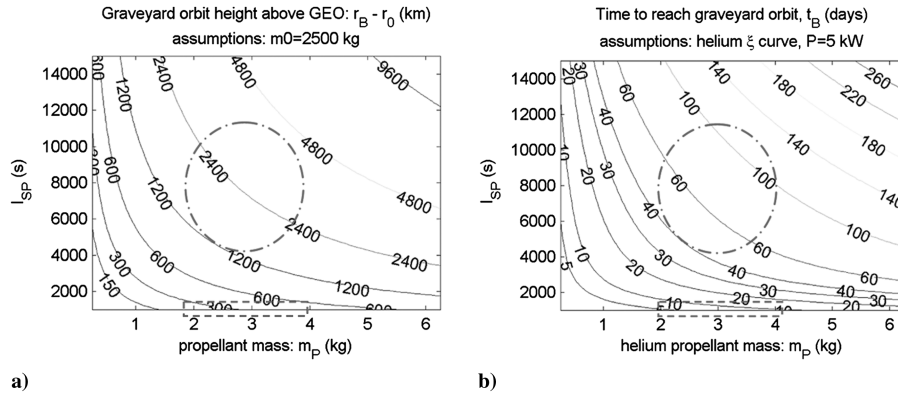


Fig. 3 a) Orbit-raising capability and b) flight times for EOL maneuver using continuous, tangent thrust; dash-dash line: operating range for helium arc jet (state of the art, see Sec. II); dash-dot line: expected range for HIT.

where a is the semimajor axis, μ is the gravitational parameter for the Earth, v is the velocity, m is the spacecraft mass, and T is the velocity direction component of the perturbing thrust. For a GEO satellite, the eccentricity is approximately zero, leading to $a = r$ and $v = (\mu/r)^{1/2}$. We assume that small perturbations (i.e., due to a low-thrust EP system) are too small to accumulate an appreciable eccentricity. We further assume that the direction of thrust is pointed entirely along the spacecraft velocity vector, the optimal energy raising direction for the zero eccentricity case. This simple control law (of full thrust aligned in the velocity direction) is near-optimal for the case of small eccentricity and leads to a simplified differential equation for radius that can be solved in closed form. Equation (6) then reduces to

$$\frac{dr}{dt} = 2 \frac{T}{m} \sqrt{\frac{r^3}{\mu}} \quad (7)$$

Equation (8) gives thrust in terms of available power P , efficiency ξ , and specific impulse I_{SP} :

$$T = 2\xi P / (g_0 I_{SP}) \quad (8)$$

Although mass is a linear function of time, given in Eqs. (9) and (10), assuming a maximum thrust level and its associated constant mass flow rate,

$$\dot{m} = -T / (g_0 I_{SP}) = -2\xi P / (g_0 I_{SP})^2 \quad (9)$$

$$m = m_0 + (\dot{m})t \quad (10)$$

The final differential equation governing radius is then

$$\frac{dr}{dt} = r^{3/2} \frac{4\xi P g_0 I_{SP}}{\sqrt{\mu}(g_0^2 I_{SP}^2 m_0 - 2\xi P t)} \quad (11)$$

with a closed-form solution:

$$r(t) = \frac{\mu r_0}{[g_0 I_{SP} \sqrt{r_0} \ln\left(1 - \frac{2\xi P t}{m_0 g_0^2 I_{SP}^2}\right) + \sqrt{\mu}]^2} \quad (12)$$

The burnout time required to burn m_p units of propellant is

$$t_B = -m_p / \dot{m} = m_p g_0^2 I_{SP}^2 / (2\xi P) \quad (13)$$

Therefore, applying $t = t_B$ to Eq. (12), the burnout radius is

$$r_B = \frac{\mu r_0}{[g_0 I_{SP} \sqrt{r_0} \ln\left(1 - \frac{m_p}{m_0}\right) + \sqrt{\mu}]^2} \quad (14)$$

Note that the efficiency and power terms affect the burnout time but are canceled in the burnout radius. Therefore, only the propellant mass fraction and the specific impulse affect the burnout radius for a given starting radius $r_0 = r_{GEO}$ and gravitational parameter $\mu = \mu_{Earth}$.

3. Orbit-Raising Capability

Using Eq. (14), Fig. 3a illustrates the expected burnout radius sensitivity to I_{SP} and propellant mass assuming an EOL spacecraft mass of 2500 kg. Using Eq. (13), Fig. 3b shows the required flight time to complete the maneuver assuming the efficiency curve from Fig. 2 and a nominal power of 5 kW. From the contours, we show representative performance for three different design points in the (m_p, I_{SP}) space in Table 2.

Figure 3 gives a preliminary performance picture of the broad design space for the HIT engine. The main assumptions of $m_0 = 2500$ kg and $P = 5$ kW are chosen conservatively, noting that GEO satellites have typical dry masses of 1500–2500 kg and power levels of 5–15 kW [22]. The nominal mass of residual helium at EOL is estimated to be 2–4 kg. This mass is a conservative estimate based on publicly available listings of the propellant tank volumes of GEO commercial satellites built by Boeing, Lockheed Martin, and Space Systems Loral [23–26]. The fuel mix, density of the fuel and oxidizer, and propellant mass lead to an estimate for a representative tank volume. Assuming an ambient temperature of 555 K and tank internal pressure of 17 atm, ideal gas law calculations reveal the estimate of the resulting helium pressurant stored in the propulsion system. The ambient temperature is intentionally selected to be high to account for a ‘worst case’ scenario; an ambient temperature of 350 K gives a range of pressurant mass between 3 and 5 kg. Considering a helium mass of 2 kg and I_{SP} of 10,000 s, the EOL maneuver is capable of raising the orbit by ~ 2200 km in ~ 2 months. An I_{sp} of 10,000 s is reasonable, given the results of the Nuclear-Electric Xenon Ion System and high-power electric propulsion ion thruster performance tests [27,28]. Therefore, we estimate the performance of the HIT engine to provide almost an order of magnitude more capability than that necessary to meet the existing graveyard orbit perigee height (GEO + ~ 250 km) requirements. This seemingly excessive HIT capability barely satisfies the 2000 km threshold given in [2] that results from evaluating explosion debris fields at GEO.

A high-fidelity low-thrust trajectory optimization is considered to verify the approximations made to produce Fig. 3. In this simulated problem, a GEO spacecraft is initiated with a circular orbit at 42,164.17 km, initial mass of 2500 kg, 2 kg of helium propellant, a 10,000 s I_{sp} helium ion thruster, and 5 kW of power, translating to an effective power of 1.84 kW (or 1.83504655 kW for reproducibility

Table 2 Representative expected performance from the HIT engine (taken from Fig. 3)

Design point	He mass, kg	I_{SP} , s	Burnout height above GEO, km	Burnout time, days
1	3	1,000	325	6.7
2	3	4,000	1320	43
3	3	8,000	2710	74
4	2	10,000	2238	61

purposes) due to the $\sim 36.7\%$ efficiency per the curve in Fig. 2. The low-thrust optimal control problem is solved using the hybrid differential dynamic programming (HDDP) method described in [29,30]. It is noted that the HDDP optimal control solver satisfies both the necessary and sufficient conditions of optimality. In this problem, the optimization procedure maximizes the final radial distance and is subject to a constraint of final eccentricity $\leq 10^{-4}$. The flight time is fixed to 60.657 days (to burn exactly 2 kg of propellant). The force model includes only the two-body Earth term plus a constant-thrust term with an unconstrained direction and a magnitude given by Eq. (8). The thrust direction is discretized to remain constant inertially across each ~ 18 min time interval, and the angular orientation of the thrust is solved in the optimal control problem. The planar transfer takes ~ 60 revolutions to complete and optimizes the thrust direction for 4865 thrusting segments. Note that the thrust magnitude is fixed at its maximum value, and the flight time is fixed to burn all of the allotted 2 kg. Therefore the typical minimum time or minimum propellant performance index is not relevant in this problem. Instead, thrust directions are optimized to maximize the final spacecraft radius subject to the low eccentricity constraint. Therefore, the solution delivers the spacecraft to the highest reachable circular graveyard orbit. Figure 4 shows the optimal time histories of the semimajor axis (with the GEO radius subtracted) as well as eccentricity and thrust angle at the end of each thrusting segment (where the angle is measured with respect to the inertial x axis). The spacecraft achieves an orbit raise above GEO by 2237.07 km compared to the 2237.91 km predicted by Eq. (14).

A second optimization is performed to give an idea of the potential tradeoff between inclination changes and orbit raising. In this example, the problem parameters are the same, except a 0.75 deg inclination change is targeted. The optimal solution raises the height above GEO by 1454.7 km and again is subject to a final eccentricity constraint of $\leq 10^{-4}$ (deemed sufficiently close to zero). The 0.75 deg inclination puts the maximum departure out of the equatorial plane at 552 km.

B. Preliminary Cost/Benefit Analysis for Incorporating the Helium Ion Thruster System

A cost-benefit analysis seeks to determine if the same capability of the HIT system can be delivered by simply adding to the existing (no HIT) satellite design the equivalent mass of the HIT system in the form of propellant. The HIT concept hinges on the fact that its helium propellant is already available. Although the HIT is less efficient than chemical thrusters, the HIT system essentially receives its propellant for free. The added launch mass is only due to the ‘dry’ HIT system

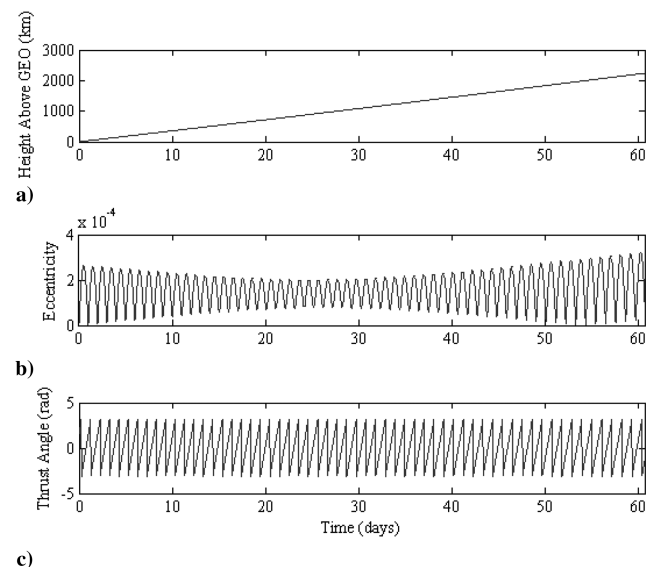


Fig. 4 High-fidelity low-thrust trajectory optimization results: a) semimajor axis, b) eccentricity, and c) thrust angle. Results plotted with time in days.

itself, m_{HIT} . With an estimate for the dry mass for the HIT system, setting the orbit-raising performance of the HIT system equal to that of an alternative system constrains how massive the dry HIT system can be and still be beneficial to the spacecraft mass budget. The right-hand side of the burnout radius expression from Eq. (14) is set equal to the same right-hand side with instead $I_{\text{SP}} = I_{\text{SP}^*}$ and $m_p = m_{\text{HIT}}$, where I_{SP^*} is for the alternative thruster, and the mass of the alternative thruster propellant is set equal to the dry mass of the HIT system. After solving for m_{HIT} and rearranging terms, we arrive at a simple equation:

$$m_{\text{HIT}} = m_0 - m_0 \left(1 - \frac{m_p}{m_0} \right)^{\frac{I_{\text{SP}}}{I_{\text{SP}^*}}} \quad (15)$$

This value for m_{HIT} represents the ‘break-even mass’ or the dry mass of the entire HIT assembly such that the ‘existing GEO satellite + HIT system with mass m_{HIT} ’ design has the same EOL orbit-raising capability as the ‘existing GEO satellite + additional m_{HIT} propellant mass using nominal thruster’ design. The break-even mass is expressed in terms of a given HIT and nominal specific impulse (I_{SP} and I_{SP^*} , respectively), EOL pre-disposal-maneuver mass m_0 , and mass of the residual helium available as propellant for the HIT. Rewriting Eq. (15) in terms of the ratios Δ and κ , we have

$$m_{\text{HIT}} = \frac{m_p}{\Delta} [1 - (1 - \Delta)^\kappa] \quad (16)$$

$$\kappa = \frac{I_{\text{SP}}}{I_{\text{SP}^*}}, \quad \Delta = \frac{m_p}{m_0} \quad (17)$$

Now, performing a Taylor series of Eq. (16) in terms of Δ and centered at $\Delta = 0$, we achieve

$$m_{\text{HIT}} = m_p \kappa - \frac{1}{2} m_p \kappa (\kappa - 1) \Delta + O(\Delta^2) + \text{H.O.T.} \quad (18)$$

Considering the size of the linear coefficient relative to the zeroth-order coefficient, it is clear that, when $\Delta(\kappa - 1)/2$ is small, the linear term bears little effect. In our application, Δ is typically $O(10^{-3})$, and κ could conceivably vary from 1 (in the case of a low-performing HIT compared to a high-performing conventional EP device) to 50 (in the case of a high-performing HIT compared to a low-performing chemical propellant). In all cases, the zeroth-order term in the Taylor series dominates, and the dependency on m_0 , is therefore removed, leaving a very simple approximation for the break-even mass:

$$m_{\text{HIT}} \approx m_p \kappa \quad (19)$$

Despite the fact that Eqs. (18) and (19) were derived using the burnout radius, Eq. (14), which assumes constant tangential thrust, the approximations in Eqs. (18) and (19) can also be shown to be valid for the case where the nominal thruster performs a two-impulse Hohmann transfer maneuver. From the rocket equation,

$$m_{\text{HIT}} = m_0 \left(1 - e^{-\frac{\delta v_H}{g_0 I_{\text{SP}^*}} \right) \quad (20)$$

where δv_H is the Hohmann velocity increment,

$$\delta v_H = \sqrt{\frac{\mu}{r_B}} \left(1 - \sqrt{\frac{2r_0}{r_0 + r_B}} \right) + \sqrt{\frac{\mu}{r_0}} \left(\sqrt{\frac{2r_B}{r_0 + r_B}} - 1 \right) \quad (21)$$

Using r_B from Eq. (14) in Eq. (21), eliminating m_0 and I_{SP^*} using the definitions of the ratios in Eq. (17), substituting the resulting δv_H into Eq. (20), and last performing a Taylor series for m_{HIT} in terms of small Δ , the simplified result is identical to that in Eq. (18). Therefore, the break-even mass approximation in Eq. (19) is valid for cost-benefit analyses when comparing the HIT performance to both low-specific-impulse chemical thrusters modeled with impulsive maneuvers and high-specific-impulse EP systems that use continuous thrust. The break-even mass is plotted in Fig. 5 for representative design points comparing to both types (chemical and EP) of nominal thruster systems.

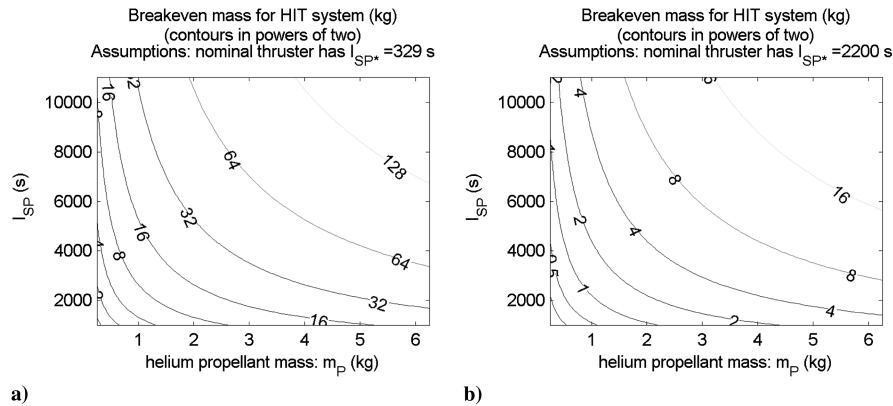


Fig. 5 Break-even mass as function of residual helium available and achieved I_{SP} for the HIT. Representative comparison to a) IHI chemical apogee engine and b) BPT-4000 Hall-effect thruster.

Considering Fig. 5a, if the HIT system using 2 kg of residual helium and producing an I_{SP} of 8000 s is compared a nominal chemical propellant thruster with 329 s I_{SP} , the break-even mass for the dry mass of the HIT system is $m_{HIT} = 48.6$ kg. Alternatively if comparing to an existing GEO satellite design that uses EP with I_{SP} of 2200 s for EOL maneuvers (but which used a chemical thruster for its initial GTO maneuver), then the same HIT design break-even mass would be much smaller at only 4 kg.

Publicly available mass estimates of gridded ion thruster systems also at the stated 5 kW design point roughly indicate the mass of a fully developed and flight qualified HIT. Two gridded ion engines that fall into the 5 kW power range are the 25 cm Xenon Ion Propulsion System (XIPS) and the 22 cm radio-frequency ion thruster (RIT). The XIPS is a conventional discharge gridded ion thruster. It has a thruster mass of 15 kg and power processing unit mass of 21.3 kg for a rough total system mass of 36 kg [31]. The RIT is an ion thruster that operates via radio-frequency excitation as opposed to discharge excitation. It has a total system mass of 28.5 kg [32]. Although the RIT is similar in operation to the HIT concept due to their mutual use of radio-frequency excitation, a conservative estimate of HIT mass using the XIPS system mass leads to a 13 kg mass advantage over the chemical break-even condition for 2 kg of helium propellant. For a system with an EP system already onboard, the addition of an HIT, given the current mass estimate, is more costly to the spacecraft mass budget than simply adding additional propellant for the EP system.

It is emphasized that the estimated mass and other point designs discussed in this paper are only speculative until an HIT system is built and tested, and further work is performed to compute the usable mass of residual helium. The true performance will be a function of several driving parameters, where the resulting broad design space is captured in this preliminary study in Figs. 3 and 5.

IV. Conclusions

In this study, a new electric propulsion device called the helium ion thruster (HIT) is proposed to simultaneously extend geosynchronous Earth orbit (GEO) satellite lifetimes and mitigate future debris risk. By leveraging helium currently used only for tank pressurization during GTO and already available on many modern GEO satellite designs, the HIT makes efficient use of a resource traditionally unused for propulsion. The proposed HIT concept is shown to enable an end-of-life (EOL) GEO satellite to be transported to an ultrasafe disposal orbit with perigee on the order of 2000 km above the GEO altitude. This perigee height, while nearly an order of magnitude higher than existing disposal guidelines, satisfies the more-stringent recommendations of a recent study that considers debris fields induced by explosions in the GEO environment. Satellite operators using the HIT architecture could completely deplete their onboard chemical propellant before considering an EOL disposal burn. Therefore, the disposal orbit burn can be removed entirely from the chemical propellant budget. Furthermore, unlike the current situation

that is plagued by poor knowledge of propellant reserves at EOL (leading to incomplete disposal maneuvers), the HIT concept ensures sufficient maneuver capability for a successful disposal. The HIT system has potential to significantly improve GEO satellite lifetimes and bring value to both government and civilian GEO spacecraft operators. The mitigation of debris population growth in the GEO band and the ability to extend operational lifetimes makes the HIT an attractive option for further study in the consideration of GEO spacecraft architectures.

References

- [1] Anselmo, L., and Pardini, C., "Space Debris Mitigation in Geosynchronous Orbit," *Advances in Space Research*, Vol. 41, No. 7, 2008, pp. 1091–1099. doi:10.1016/j.asr.2006.12.018
- [2] Anselmo, L., and Pardini, C., "Collision Risk Mitigation in Geostationary Orbit," *Space Debris*, Vol. 2, No. 2, 2000, pp. 67–82. doi:10.1023/A:1021255523174
- [3] Rudiger, J., Agapov, V., and Hernández, C., "End-of-Life Disposal of Geostationary Satellites," 4th European Conf. on Space Debris, Darmstadt, Germany, edited by D. Danesy, European Space Agency SP 587, April 2005.
- [4] Payne, T., and Morris, R., "The Space Surveillance Network (SSN) and Orbital Debris," *33rd Annual AAS Guidance and Control Conf.*, Breckenridge, CO, American Astronautical Society Paper 10-012, Feb. 2010.
- [5] Liou, J. C., *Orbital Debris Quarterly News*, Vol. 15, No. 1, Jan. 2011, p. 10.
- [6] Hoffman, M., "It's Getting Crowded Up There," *Space News*, 3 April 2009.
- [7] Kessler, D. J., and Cour-Palais, B. G., "Collision Frequency of Artificial Satellites: The Creation of a Debris Belt," *Journal of Geophysical Research*, Vol. 83, No. A6, pp. 2637–2646. doi:10.1029/JA083iA06p02637
- [8] Achenbach, J., "Astronauts Evacuate Space Station Temporarily During Collision Scare," *Washington Post*, 13 March 2009.
- [9] Osborn, A., "International Space Station Evacuated After Debris Threatens Craft," *The Telegraph*, 28 Jun 2011.
- [10] Hyde, J. L., Christiansen, E. L., Bernhard, R. P., Kerr, J. H., and Lear, D. M., "A History of Meteoroid and Orbital Debris Impacts on the Space Shuttle," *Proceedings of the 3rd European Conference on Space Debris*, Darmstadt, Germany, ESA Publications Division, Noordwijk, Netherlands, March 2001, pp. 191–196.
- [11] Power, J. L., "Microwave Electrothermal Propulsion for Space," *IEEE Transactions on Microwave Theory and Techniques*, Vol. 40, No. 6, June 1992, pp. 1179–1191. doi:10.1109/22.141350
- [12] Welle, R. P., Pollard, J. E., Janson, S. W., Crofton, M. W., and Cohen, R. B., "One Kilowatt Hydrogen and Helium Arcjet Performance," *AIAA/SAE/ASME/ASEE Joint Propulsion Conf.*, Sacramento, CA, AIAA Paper 1991-2229, June 1991.
- [13] Whitehair, S., Asmussen, J., and Nakanishi, S., "Demonstration of a New Electrothermal Thruster Concept," *Applied Physics Letters*, Vol. 44, May 1984, pp. 1014–1016. doi:10.1063/1.94603
- [14] Mueller, J., and Micci, M. M., "Microwave Electrothermal Thrusters

- Using Waveguide Heated Plasmas,” 21st AIAA/DGLR/JSASS International Electric Propulsion Conf., Orlando, FL, AIAA Paper 1990-2562, July 1990.
- [15] Diamant, K. D., “Microwave Electrothermal Thruster Performance,” *Journal of Propulsion and Power*, Vol. 23, No. 1, Jan.–Feb. 2007, pp. 27–34.
doi:10.2514/1.19571
- [16] Souliez, F. J., Chianese, S. G., Dizac, G. H., and Micci, M. M., “Low-Power Microwave Arcjet Testing: Plasma and Plume Diagnostic and Performance Evaluation,” *Micropropulsion for Small Spacecraft*, edited by M. M. Micci and A. D. Ketsdever, Vol. 187, Progress in Astronautics and Aeronautics, AIAA, Reston, VA, 2000, pp. 199–214.
- [17] Welle, R. P., “Space Propulsion Applications of Helium Arcjets,” DTIC SMC-TR-00-13, 2000, pp. 1–13.
- [18] Rybakov, A., Auweter-Kurtz, M., Kurtz, H., and Riehle, M., “Investigations of the 1 kW Class Arcjet ARTUR-2 with Helium as Propellant,” 38th AIAA/ASME/SAE/ASEE Joint Propulsion Conf. and Exhibit, Indianapolis, IN, AIAA Paper 2002-3659, July 2002.
- [19] Ahedo, E., Martinez-Cerezo, P., and Martinez-Sanchez, M., “One-Dimensional Model of the Plasma Flow in a Hall Thruster,” *Physics of Plasmas*, Vol. 8, No. 6, 2001, pp. 3058–3068.
doi:10.1063/1.1371519
- [20] Jahn, R. G., *Physics of Electric Propulsion*, Vol. 1, McGraw–Hill, 1968, pp. 142–195.
- [21] Battin, R. H., *An Introduction to the Mathematics and Methods of Astrodynamics*, AIAA, New York, 1987, p. 489.
- [22] Spence, B. R., Jones, P. A., Eskenazi, M. I., and Murphy, D. M., “The SCARLET Solar Array for High Power GEO Satellites,” *IEEE Photovoltaic Specialists Conf.*, IEEE Publ., Piscataway, NJ, 1997, pp. 1027–1030.
- [23] “AS 2100,” *Encyclopedia Astronautica*, <http://www.astronautix.com/craft/as2100.htm> [retrieved 23 September 2011].
- [24] “FS-1300,” *Encyclopedia Astronautica*, <http://www.astronautix.com/craft/fs1300.htm> [retrieved 23 September 2011].
- [25] “HS 702,” *Encyclopedia Astronautica*, <http://www.astronautix.com/craft/hs702.htm> [retrieved 23 September 2011].
- [26] Arcioni, M., Daehler, E., Mueller, R. P., and van der Muelen, W., “S@tMax—A Space-Based System Enabling Mobile IP Applications in Vehicles,” *Acta Astronautica*, Vol. 64, pp. 1167–1179.
doi:10.1016/j.actaastro.2009.01.028
- [27] Goebel, D. M., Polk, J., and Sengupta, A., “Discharge Chamber Performance of the NEXIS Ion Thruster,” 40th AIAA/ASME/SAE/ASEE Joint Propulsion Conference and Exhibit, Fort Lauderdale, FL, AIAA Paper 2004-3813, July 2004.
- [28] Foster, J. E., Haag, T., Patterson, M., Williams, G. J. Jr., Sovey, J. S., Carpenter, C., et al., “The High Power Electric Propulsion (HiPEP) Ion Thruster,” 40th AIAA/ASME/SAE/ASEE Joint Propulsion Conference and Exhibit, Fort Lauderdale, FL, AIAA Paper 2004-3812, July 2004.
- [29] Lantoine, G., and Russell, R. P., “A Hybrid Differential Dynamic Programming Algorithm for Constrained Optimal Control Problems, Part 1: Theory,” *Journal of Optimization Theory and Applications*, Vol. 154, No. 2, 2012, pp. 382–417.
doi: 10.1007/s10957-012-0039-0
- [30] Lantoine, G., and Russell, R. P., “A Hybrid Differential Dynamic Programming Algorithm for Constrained Optimal Control Problems, Part 2: Applications,” *Journal of Optimization Theory and Applications*, Vol. 154, No. 2, 2012, pp. 418–442.
doi: 10.1007/s10957-012-0038-1
- [31] Chien, K., Hart, S. L., Tighe, W. G., De Pano, M. K., Bond, T. A., and Spears, R., “L-3 Communications ETI Electric Propulsion Overview,” 29th AIAA/DGLR/JSASS International Electric Propulsion Conference, IEPC Paper 2005-315, Princeton, NJ, Oct. 2005.
- [32] Dachwald, B., Seboldt, W., Loeb, H. W., and Schartner, K. H., “Main Belt Asteroid Sample Return Mission Using Solar Electric Propulsion,” *Acta Astronautica*, Vol. 63, pp. 91–101.
doi:10.1016/j.actaastro.2007.12.023

J. Blandino
Associate Editor